Journal of Applied Fluid Mechanics, Vol. 9, No. 1, pp. 451-461, 2016.
Available online at www.jafmonline.net, ISSN 1735-3572, EISSN 1735-3645.

Investigation of Three-Dimensional Axisymmetric Unsteady Stagnation-Point Flow and Heat Transfer Impinging on an Accelerated Flat Plate

A. Shokrgozar [1 †], A. B. Rahimi [2] and H. Mozayyeni

[1] *Department of mechanical engineering, Payame Noor University, Iran*
[2] *Faculty of Engineering, Ferdowsi University of Mashhad, Mashhad, Iran*

†*Corresponding Author Email:shokrgozar.ali@gmail.com*

(Received December 14, 2014; accepted February 5, 2015)

ABSTRACT

General formulation and solution of Navier-Stokes and energy equations are sought in the study of three-dimensional axisymmetric unsteady stagnation-point flow and heat transfer impinging on a flat plate when the plate is moving with variable velocity and acceleration towards the main stream or away from it. As an application, among others, this accelerated plate can be assumed as a solidification front which is being formed with variable velocity. An external fluid, along z - direction, with strain rate a impinges on this flat plate and produces an unsteady three-dimensional axisymmetric flow in which the plate moves along z - direction with variable velocity and acceleration in general. A reduction of Navier-Stokes and energy equations is obtained by use of appropriate similarity transformations, for the first time. The obtained ordinary differential equations are solved by using finite-difference numerical techniques. Velocity and pressure profiles along with temperature profiles are presented for different examples of the plate velocity functions and selected Prandtl numbers. According to the results obtained, the velocity and thermal boundary layers feel the effect of variations of the plate velocity more than the plate acceleration. It means that the minimum boundary layer thickness happens at the maximum value of the plate velocity and acceleration effect plays a secondary role.

Keywords: Stagnation-point flow and heat transfer; Unsteady flow; Viscous fluid; Accelerated plate; Similarity solution; Three-dimensional axisymmetric.

NOMENCLATURE

$a(t)$	time-dependent flow strain rate
a_o	flow strain rate at time=0
$\tilde{a}(\tau)$	dimensionless strain rate
h	heat transfer coefficient
H	dimensionless heat transfer coefficient
k	thermal conductivity of the fluid
p	pressure
$\tilde{P}$	dimensionless pressure
Pr	prandtl number
T	temperature
S, $\dot{S}$, $\ddot{S}$	displacement, velocity and acceleration of the plate, respectively, in z-direction
$\tilde{S}$, $\tilde{\dot{S}}$, $\tilde{\ddot{S}}$	dimensionless, velocity and acceleration of the plate respectively, in z-direction
u, w	velocity components near the plate in r, z directions
U, W	potential region velocity components in r, z directions r, z cylindrical coordinates
β	volumetric expansion coefficient
η	similarity variable
μ	dynamic viscosity
θ	dimensionless temperature
σ	shear stress
$\tilde{\sigma}$	dimensionless shear stress
τ	dimensionless time
ζ	variable $(z - S(t))$
ξ	dimensionless r-axis
ρ	density
υ	kinematic viscosity

Subscripts

o	stagnation point	∞	infinite
		w	wall

1. INTRODUCTION

Many solutions of Navier-Stokes and energy equations regarding the problem of stagnation-point flow and heat transfer in the vicinity of a flat plate or a cylinder are found in the literature for different cases. Removing the nonlinearity in these problems is usually accomplished by superposition of fundamental exact solutions that lead to a coupled system of nonlinear ordinary differential equations. Fundamental studies in which flows are readily superposed and/or the axisymmetric case were considered include the following papers presented in the literature: uniform shear flow over a flat plate in which the flow is induced by a plate oscillating in its own plane beneath a quiescent fluid (Stokes 1851); two-dimensional stagnation-point flow (Hiemenz 1911); flow over a flat plate with uniform normal suction (Griffith and Meredith 1936); three-dimensional stagnation-point flow (Homman 1936); and axisymmetric stagnation flow on a circular cylinder (Wang 1974). Further exact solutions to the Navier-Stokes equations are obtained by superposition of the uniform shear flow and/or stagnation flow on a body oscillating or rotating in its own plane or cylinder, with or without suction. The examples are: superposition of two-dimensional and three-dimensional stagnation-point flows (Howarth 1954); superposition of uniform suction at the boundary of a rotating disk (Stuart 1954); also the solution for a fluid oscillating about a nonzero mean flow parallel to a flat plate with uniform suction given (Stuart 1955); superposition of stagnation-point flow on a flat plate oscillating in its own plane, and also consideration of the case where the plate is stationary and the stagnation stream is made to oscillate (Glauert 1956); uniform shear flow aligned without flowing two-dimensional stagnation-point flow (Stuart 1959); uniform flow along a flat plate with time-dependent suction and included periodic oscillations of the external stream (Kelly 1965); heat transfer in an axisymmetric stagnation flow on a cylinder (Gorla 1976); unsteady laminar axisymmetric stagnation flow over a circular cylinder (Gorla 1977); nonsimilar axisymmetric stagnation flow on a moving cylinder (Gorla 1978); transient response behavior of an axisymmetric stagnation flow on a circular cylinder due to time-dependent free stream velocity (Gorla 1978); unsteady viscous flow in the vicinity of an axisymmetric stagnation-point on a cylinder (Gorla 1979); shear flow over a rotating plate (Wang 1989); radial stagnation flow on a rotating cylinder with uniform transpiration (Cunning, Davis, and Weidman 1998); suppression of turbulence in wall-bounded flows by high-frequency span wise oscillations (Jung and Mangiavacchi 1992); axisymmetric stagnation flow towards a moving plate (Wang 1973); oscillating stagnation-point flow (Grosch and Salwen 1982); unsteady axisymmetric stagnation-point flow of a viscous fluid on a cylinder (Takhar and Chamkha 1999); axisymmetric stagnation-point flow and heat transfer of a viscous fluid on a moving cylinder with time-dependent axial velocity and uniform transpiration (Saleh and Rahimi 2004); axisymmetric stagnation-point flow and heat transfer of a viscous fluid on a rotating cylinder with time-dependent angular velocity and uniform transpiration (Rahimi and Saleh 2007); similarity solution of un-axisymmetric heat transfer in stagnation-point flow on a cylinder with simultaneous axial and rotational movements (Rahimi and Saleh 2008); Non-axisymmetric three-dimensional stagnation-point flow and heat transfer on a flat plate (Shokrgozar and Rahimi 2009); and three-dimensional stagnation flow and heat transfer on a flat plate with transpiration (Shokrgozar and Rahimi 2009). Moreover, exact solutions for the problems of unsteady stagnation-point flow over a vertically moving plate for both axisymmetric and two-dimensional cases in Ref. (Zhong and Fang 2011); non-axisymmetric stagnation-point flow by adding radial and azimuth velocities (Weidman 2012); and steady three-dimensional stagnation flow and heat transfer of a viscous, compressible fluid on a flat plate in Ref. (Mozayyeni and Rahimi 2013) were recently published.

Among all the studies above only in References (Grosch and Salwen 1982; Zhong and Fang 2011) the flat plate has a vertical movement. In Ref. (Grosch and Salwen 1982), the plate oscillates in the vertical direction. In this paper, some particular solutions have been obtained by use of Fourier's expansions. Besides, in Ref. (Zhong and Fang 2011) in order for a similarity solution to be attained both the free stream velocity and the plate velocity varies with specific, time-dependent functions. A two-dimensional study of a plate with vertical movement has also been submitted as a technical brief as Ref. (Shokrgozar and Rahimi 2012). Consequently, similarity solution of three-dimensional stagnation-point flow and heat transfer problem on a flat plate with arbitrary vertical movement is non-existing in the literature.

In this study the general unsteady three-dimensional axisymmetric viscous stagnation-point flow and heat transfer in the vicinity of a flat plate are investigated where this flat plate is moving towards or away from the impinging flow with variable velocity and acceleration. The Navier-Stokes equations along with energy equation are solved. The importance of this research work is encountered in problems where the solid participant is moving towards the impinging flow, for example in solidification in which the solid front is growing. The external fluid impinges on this flat plate along z-direction, with strain-rate a, while the plate is moving with variable velocity and acceleration along z-direction. Appropriate similarity transformations are used to reduce the Navier-

Stokes and energy equations to a coupled system of ordinary differential equations. The results are presented for different examples of the plate velocity functions and selected Prandtl numbers.

2. PROBLEM FORMULATION

Flow is considered in cylindrical coordinates (r,z) with corresponding velocity components (u,w), see Fig. 1. We consider the unsteady laminar incompressible flow and heat transfer of a viscous fluid in the neighborhood of stagnation-point on a moving flat plate located in the plane $z=0$ at $t=0$. The plate can move with any arbitrarily time-dependent velocity and acceleration functions. An external fluid flow approaches the plate along the opposite direction of z-axis, with strain -rate a, and impinges on this accelerated plate. Afterwards, the flow divides and moves away from the stagnation point along the wall radially in all directions. In this axisymmetric case, r-direction is to be considered as cylindrical radius coordinate. As an application, this accelerated plate can be assumed as a solidification front which is moving with variable velocity along the z-axis in which the solid thickness is growing steadily in r direction.
For a Newtonian fluid with constant density and viscosity, unsteady Navier-Stokes and energy equations in cylindrical coordinates governing the flow and heat transfer are given as:

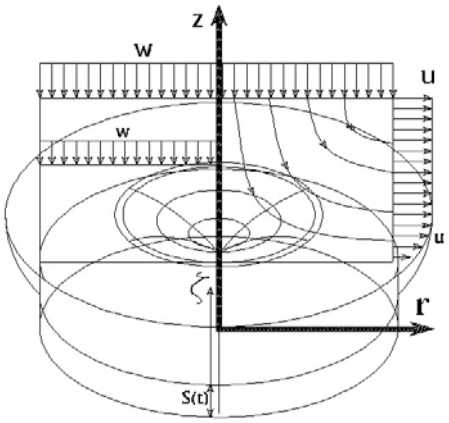

Fig. 1. Schematic Problem Graph.

Mass:

$$\frac{1}{r}\frac{\partial}{\partial r}(ru)+\frac{\partial w}{\partial z}=0 \tag{1}$$

Momentum:

$$\frac{\partial u}{\partial t}+u\frac{\partial u}{\partial r}+w\frac{\partial u}{\partial z}= =-\frac{1}{\rho}\frac{\partial p}{\partial r}+\upsilon\left(\frac{\partial^2 u}{\partial r^2}+\frac{1}{r}\frac{\partial u}{\partial r}-\frac{u}{r^2}+\frac{\partial^2 u}{\partial z^2}\right) \tag{2}$$

$$\frac{\partial w}{\partial t}+u\frac{\partial w}{\partial r}+w\frac{\partial w}{\partial z} =-\frac{1}{\rho}\frac{\partial p}{\partial z}+\upsilon\left(\frac{\partial^2 w}{\partial r^2}+\frac{1}{r}\frac{\partial w}{\partial r}+\frac{\partial^2 w}{\partial z^2}\right) \tag{3}$$

Energy (dissipation and radiation heat transfer are neglected without internal source):

$$\frac{\partial T}{\partial t}+u\frac{\partial T}{\partial r}+w\frac{\partial T}{\partial z}=\alpha\left[\frac{\partial^2 T}{\partial r^2}+\frac{1}{r}\frac{\partial T}{\partial r}+\frac{\partial^2 T}{\partial z^2}\right] \tag{4}$$

Notice conductivity and heat capacity coefficients are constant (k and c respectively) also $du \approx c\,dT$ is assumed where p, ρ, υ, and α are the fluid pressure, density, kinematic viscosity, and thermal diffusivity.

3. SIMILARITY SOLUTION

3.1 Fluid Flow Solution

The classical potential flow solution of the governing equations (1)-(3) is as follows ((Weidman 2012) without azimuth velocity):

$$U=a(t)r \tag{5}$$

By inserting (5) in continuity equation and after integrating:

$$W=-2a(t)\,\zeta \tag{6}$$

Where $\zeta=z-S(t)$ and $S(t)$ is the amount of plate displacement in z- direction and is assumed to be positive when the plate moves toward the impinging flow. Hence, $S(t)$ and, then, ζ are functions of time. According to the definition of flow strain-rate $a(t)=\partial w/\partial\zeta$, $a(t)$ can be, also, expressed as a time-dependent function in problems comprising moving plate with time-dependently variable velocity and acceleration.

A reduction of the Navier-Stokes equations is sought by the following coordinate separation in which the solution of the viscous problem inside the boundary layer is obtained by composing the inviscid and viscous parts of the velocity components (Shokrgozar and Rahimi 2009):

$$u=a(t)\,r\,f'(\eta) \tag{7}$$

$$w=-2\sqrt{\upsilon/a_\circ}\;a(t)\,f(\eta) \tag{8}$$

$$\eta=\sqrt{\upsilon/a_\circ}\,\zeta \quad ,and \quad \zeta=z-S(t) \tag{9}$$

Where terms involving $f(\eta)$ in (7), (8) comprise the cylindrical similarity form for unsteady stagnation-point flow and prime denotes differentiation with respect to η. Moreover, $a_\circ$ is the reference potential flow strain- rate at the time=0. Note, boundary layer is defined here as the edge of the points where their velocity is 99% of their corresponding potential velocity. Transformations (7)-(9) satisfy (1) automatically and their insertion into (2) - (3) yields an ordinary

differential equation in terms of $f(\eta)$ and an expression for the pressure:

$$f''' + f''\left(\tilde{\dot{S}} + 2\tilde{a}\, f\right) + \left(-\tilde{a}\, f' - \frac{1}{\tilde{a}}\frac{d\tilde{a}}{d\tau}\right) f' - \frac{1}{\tilde{a}}\,\xi\,\frac{\partial \tilde{P}}{\partial \xi} = 0 \tag{10}$$

$$\text{,where } -\frac{1}{\tilde{a}}\,\xi\,\frac{\partial \tilde{P}}{\partial \xi} = \frac{1}{\tilde{a}}\frac{\partial \tilde{a}}{\partial \tau} + \tilde{a}$$

$$\tilde{p} - \tilde{p}_\circ = -2\tilde{a}\left(\tilde{a} f^2 + f' + \tilde{\dot{S}} f\right) - \frac{\xi^2}{2}\left(\frac{\partial \tilde{a}}{\partial \tau} + \tilde{a}^2\right) + \int_0^\eta 2\frac{\partial \tilde{a}}{\partial \tau}\, f\, d\eta \tag{11}$$

Where:

$$\tilde{a}(\tau) = a(t)/a_\circ\,,\quad \tilde{P} = p/\left(\rho_\infty a_\circ \upsilon_\infty\right),\ \tau = a_\circ t$$
$$\tilde{S}(t) = \sqrt{a_\circ \upsilon_\infty}\, S(t)\,,\quad \tilde{\dot{S}} = \dot{S}/\sqrt{a_\circ \upsilon_\infty}$$
$$\tilde{\ddot{S}} = \ddot{S}/\left(a_\circ \sqrt{a_\circ \upsilon_\infty}\right),\quad \xi = r\sqrt{a_\circ \upsilon_\infty} \tag{12}$$
$$\frac{\partial \tilde{a}}{\partial \tau} = \frac{\tilde{\ddot{S}}}{\eta_\circ} + \frac{\tilde{\dot{S}}^2}{\eta_\circ^2} + \frac{\tilde{W}_\circ \tilde{\dot{S}}}{\eta_\circ^2}$$

In which, "dot" in dimensionless parameters denotes differentiation with respect to τ and quantities $\tilde{a}(\tau), \tilde{P}, \tilde{P}_\circ, \tau, \tilde{\dot{S}}, \tilde{\ddot{S}}$ and ξ are non-dimensional forms of quantities strain- rate, pressure, stagnation pressure, time, plate velocity, plate acceleration and r, respectively. Also, $\eta_\circ$ is the vertical distance from the plate in which the incoming potential flow starts feeling the movement of the plate. The quantity $\tilde{W}_\circ$ is dimensionless velocity of potential impinging flow at $\eta_\circ$. Relation (11) which represents pressure is obtained by integrating Eq. (3) in z-direction and by use of the potential flow solution (5) - (6) as boundary conditions. Here, Eq. (10) is in the most general form for any arbitrary flat plate vertical movement and the boundary conditions for this equation are:

$$\eta = \circ: \quad f = 0,\quad f' = 0 \tag{13}$$

$$\eta \to \infty: \quad f' = 1 \tag{14}$$

Note that, in steady-state conditions in which the plate velocity and acceleration are zero, $\left(\dot{S} = 0\ \&\ \ddot{S} = 0\right) a(t) = a_\circ$ and Eq. (10) simplifies to the case of Homann flow obtained in Ref. (Homman 1936) which is the three-dimensional case of Hiemenz flow, Ref. (Hiemenz 1911).

Shear- stress at the wall surface is given by,

$$\sigma = \mu\ \partial u/\partial z\big|_{z=0} \tag{15}$$

On applying dimensionless parameters defined in section 3, dimensionless form of shear- stress on the flat plate is presented by,

$$\tilde{\sigma} = \xi\ f''\big|_\eta \quad \text{where,}\ \ \tilde{\sigma} = \sigma/\left(\rho a_\circ \upsilon\right) \tag{16}$$

3.2 Heat Transfer Solution:

To transform the energy equation into a non-dimensional form for the case of defined wall temperature, we introduce:

$$\theta = \frac{T(\eta) - T_\infty}{T_w - T_\infty} \tag{17}$$

Making use of transformations (7) - (9), this equation may be written as:

$$\theta'' + \left(\tilde{\dot{S}}(\tau) + 2\tilde{a}\, f\right) \mathrm{Pr}.\theta' = 0 \tag{18}$$

With boundary conditions as:

$$\eta = 0: \qquad \theta = 1 \tag{19}$$

$$\eta \to \infty: \qquad \theta = 0 \tag{20}$$

Where θ is dimensionless temperature, the subscript w and ∞ refer to the conditions at the wall and in the free stream, respectively, $\mathrm{Pr} = \upsilon/\alpha$, is Prandtl number and prime indicates differentiation with respect to η.

The local heat transfer coefficient on the flat plate is calculated from,

$$h = q_w/\left(T_w - T_\infty\right) \tag{21}$$

Using the relation (19) and dimensionless parameters, the dimensionless form of the heat transfer coefficient for this study can be gained as,

$$H = -\theta'\big|_{\eta=0} \quad \text{,Where } H = h/\left(k\sqrt{a/\upsilon}\right) \tag{22}$$

4. PRESENTATION OF RESULTS

In order to validate the results obtained, f' distributions are compared with those of reference (Mozayyeni and Rahimi 2013) for the case of stationary plate $(\tilde{\dot{S}} = 0.0)$. As it can be seen from Fig. 2, there is no difference for this quantity comparing with Ref. (Shokrgozar and Rahimi 2012).

As examples, the following three distinct velocity functions are considered:

$$\tilde{\dot{S}}(\tau) = \exp(-\tau) \tag{23}$$

$$\tilde{\dot{S}}(\tau) = \tau^2 \tag{24}$$

$$\tilde{\dot{S}}(\tau) = \cos(\tau) \tag{25}$$

The exponential velocity function above, for example, can be used to model the physical one or three-dimensional solidification problem. Equation (10) for a known plate velocity function is an ordinary differential equation and can be solved numerically along with Eq. (16) by using a shooting method trial and error and based on the Runge-

Kutta algorithm. This procedure is applied for maximum error of less than 0.00001.

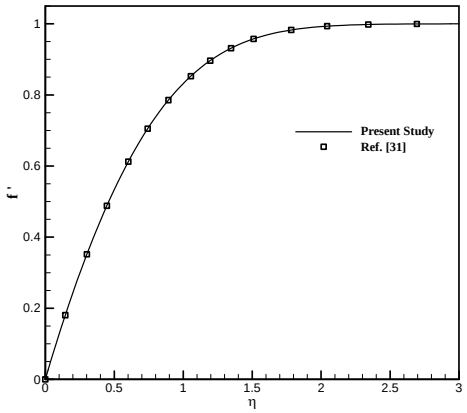

Fig. 2. Comparison of f' profiles with Ref. (Mozayyeni and Rahimi 2013) for stationary plate $(\tilde{S} = 0.0)$.

In Figs. 3-5, the boundary layer velocity profile in r direction for exponential, polynomial and co sinusoidal, respectively, plate velocity functions in different time values are shown. As it can be seen in Fig. 3, when the time increases, the f' values decrease in the region close to the plate. It is important to note that with the passing of time, the plate velocity and acceleration approaches zero.

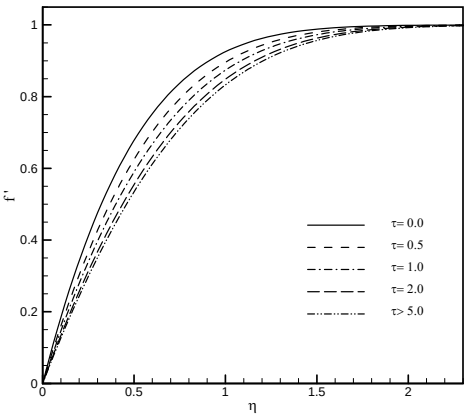

Fig. 3. distribution of f' at different times for Exponential plate velocity function.

Hence, the velocity profile gradually tends toward the Homann flow. If the plate moves with the polynomial velocity function, Fig.4, the increase of time causes the boundary layer thickness to decrease considerably. In Fig. 5, the plate is assumed to be moved with a co sinusoidal velocity function. As we know, at the time 0, the plate velocity has the value of +1, i.e. moving with the highest speed toward the impinging flow. As the time goes by, the velocity reduces until gets the value of -1 at the time π, i.e. moving with the highest speed away from the incoming potential flow.

The decrease in the velocity value in this time duration causes the f' boundary layer thickness to increase. If the passing of time is continued from π to 2π, the value of the plate velocity increases gradually from -1 to +1 and brings about the change in the direction of the plate movement. This phenomenon causes the decrease in the boundary layer thickness, as expected.

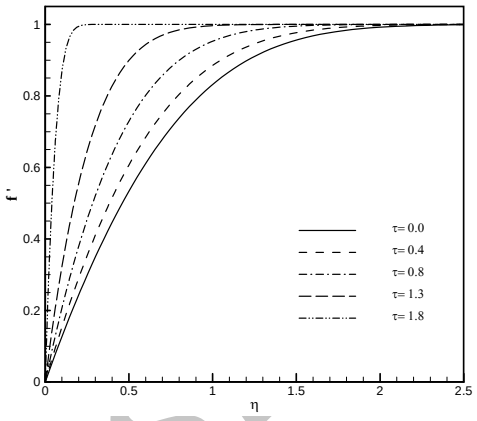

Fig. 4. distribution of f' at different times for Polynomial plate velocity function.

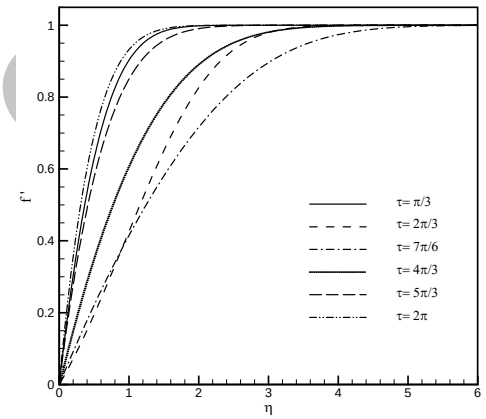

Fig. 5. distribution of f' at different times for co sinusoidal plate velocity function.

The effect of time on dimensionless distribution of w velocity component is illustrated in Figs. 6 to 8 for selected velocity functions. For an exponentially moving plate, Fig. 6, with the increase of the time the velocity component in z-direction decreases. In contrast, if the plate moves with polynomial function, the f values are growing in the vicinity of the plate as the time passes. It is because of the increase in the velocity and acceleration of the plate. For the case of co sinusoidal movement, the more the time departures from 0 to π, the higher values are captured for z-direction velocity component. If the passage of time is continued, from π to 2π, the f function values are decreased, gradually, until reach the lowest ones at the time 2π.

The dimensionless pressure distributions are depicted in Figs. 9 and 10 for moving plate with exponential and co sinusoidal, respectively, velocity

functions. According to Fig. 9, the passage of time causes the decrease in the absolute values of pressure in the region close to the plate. This feature is more dominated at the beginning of the motion. For the case of co sinusoidal movement, one can see the sample results for pressure distributions in one periodic motion over a time period of 0 to 2π.

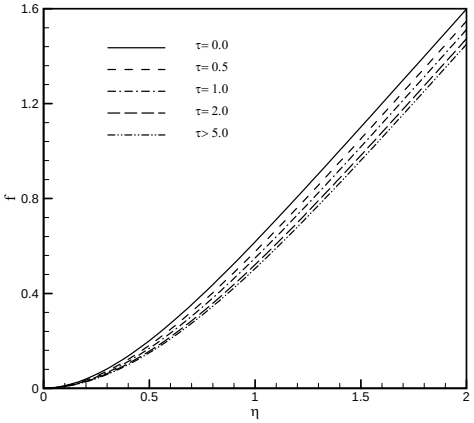

Fig. 6. f function distribution at different times for Exponential plate velocity function.

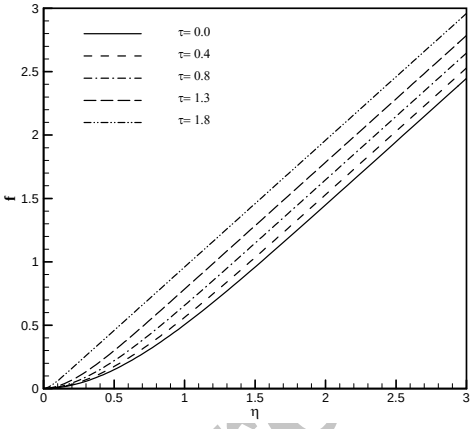

Fig. 7. f function distribution at different times for Polynomial plate velocity function.

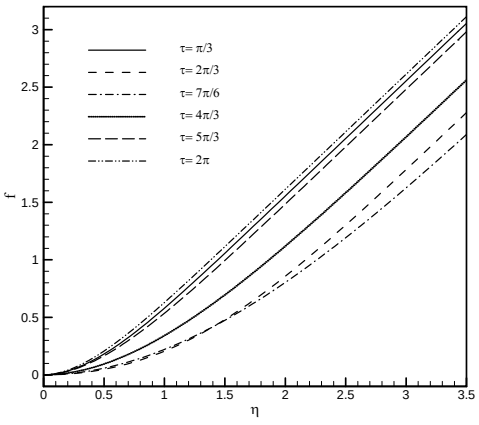

Fig. 8. f function distribution at different times for co sinusoidal plate velocity function.

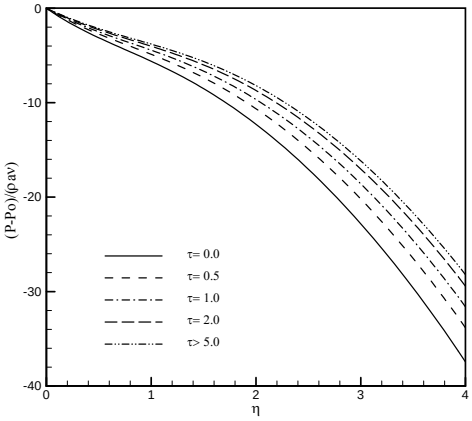

Fig. 9. Pressure distribution at different times for Exponential plate velocity function.

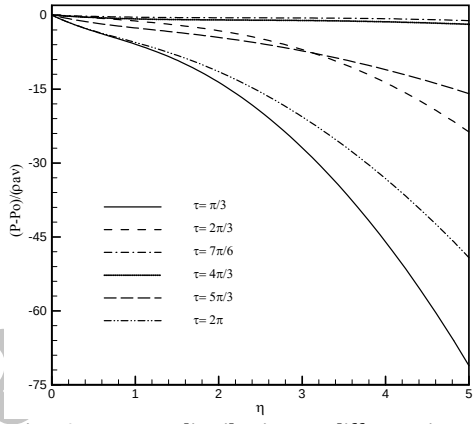

Fig. 10. Pressure distributions at different times for co sinusoidal plate velocity function.

In Figs. 11 and 12, the thermal boundary layer profiles are shown for exponential plate velocity function and selected values of Pr number, 0.1 and 20. Not many considerable changes are reported for temperature distributions of a fluid with Pr number 0.1 when the time passes, Fig. 11. In contrast, the thermal boundary layer thickness decreases rapidly with the passage of time, for a fluid with high-valued Pr number. Besides, Figs.13 and 14 depict the temperature distributions with respect to time in the vicinity of the plate for the case of polynomial velocity function and for selected Pr numbers 0.1 and 20. As it can be noticed, the increase of time brings about the decrease of the thermal boundary layer thickness for any value of Pr number. Moreover, it can be found out by comparing these two figures that the thermal boundary layer thickness becomes smaller noticeably if the Pr number gets higher values. Figure 15, shows temperature distributions at different times when the velocity of the plate obeys the co sinusoidal function. According to this figure, when the time departures from 0 to π the thermal boundary layer is growing continuously. However, the thermal boundary layer thickness starts decreasing when the passage of time is continued from π to 2π.

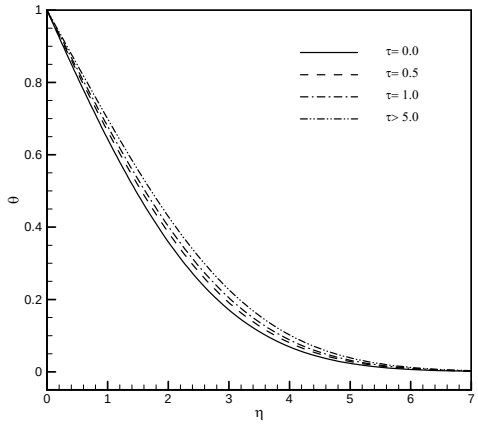

Fig. 11. Temperature distributions at different times for Exponential plate velocity function when.
Pr =0.1

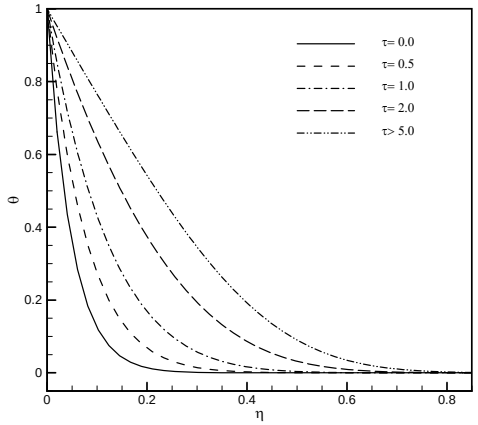

Fig. 12. Temperature distributions at different times for Exponential plate velocity function when.
Pr =20

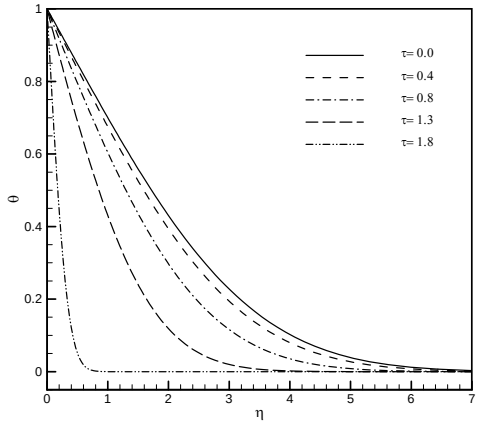

Fig.13. Temperature distributions at different times for Polynomial plate velocity function when.
Pr =0.1

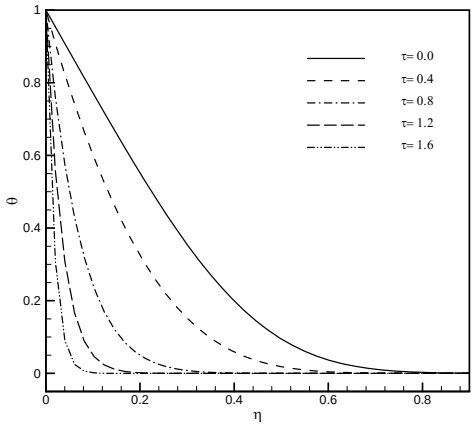

Fig. 14. Temperature distributions at different times for Polynomial plate velocity function when.
Pr =20

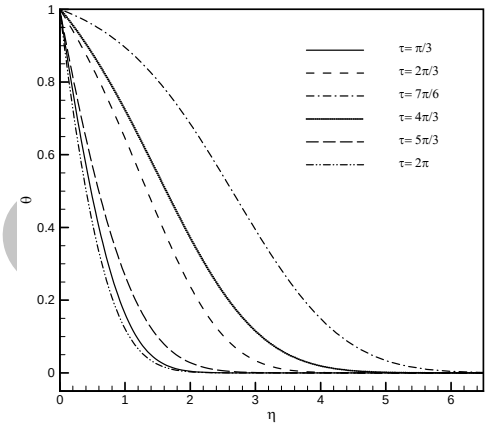

Fig. 15. Temperature distribution at different times for co sinusoidal plate velocity function when.
Pr=1

The effect of passage of time on distributions of dimensionless heat transfer coefficient is illustrated for different values of Prandtl number when the plate moves toward the impinging flow with an exponential velocity function, Fig. 16, and with a polynomial velocity function, Fig. 17. For an exponentially moving plate, the increase of time at the outset causes the noticeable decrease in the amount of heat transfer coefficient. This trend continues until reaching a constant value at steady-state condition. It should be noted that, the more the Pr number the more the coefficient H will be at any selected time. As it was discussed in Figs. 13 and 14, if the plate moves toward the impinging flow with a polynomial velocity function, the temperature gradient of the fluid increases with increase of τ in the region close to the plate. According to Eq. 20, as the temperature gradient increases the dimensionless heat transfer coefficient increases as well. This phenomenon has been illustrated in Fig. 17. According to this figure, the H coefficient consistently enhances with increase of τ. This enhancement is much more considerable if the

Pr number of the fluid is high.

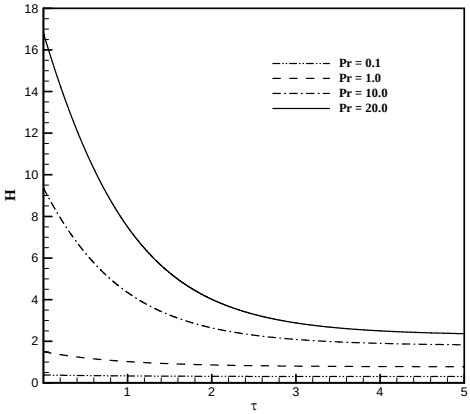

Fig. 16. Distributions of H coefficient with respect to time for exponential plate velocity function for different values of Pr numbers.

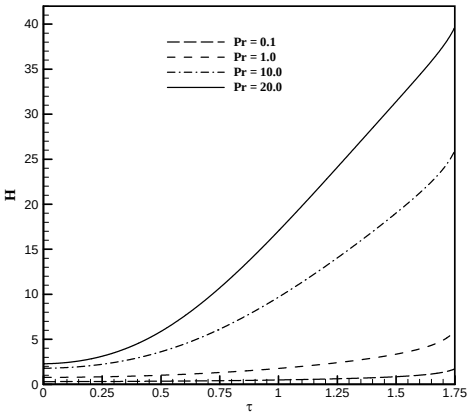

Fig. 17. Distributions of H coefficient with respect to time for polynomial plate velocity function for different values of Pr numbers.

In Fig. 18, the distribution of shear- stress on the plate is presented when the plate velocity varies with time with exponential and polynomial functions. As it can be seen in this figure, the trend of shear- stress change is completely different for these two velocity functions. With the passage of time, an exponentially moving plate approaches the steady- state condition. Consequently, the shear-stress decreases gradually to reach a consistent value which is 1.313. It is worth noting that this value is close enough with that of Ref. (Zhong *et al*, 2011). Hence, it can be considered as another validation criterion. In contrast, as it was seen in Fig. 4, if the velocity of the plate varies with a polynomial function, the velocity gradient in viscous boundary layer increases considerably with enhancement of τ. As a result, shear-stress on the plate increases with a high rate as time passes.

5. CONCLUSIONS

General formulation and similarity solution of the Navier-Stokes and energy equations have been derived in the study of axisymmetric three-dimensional unsteady stagnation-point flow and heat transfer impinging on a flat plate where this plate is moving with arbitrary velocity and acceleration functions of time towards the main stream or away from it. The results of the stagnation-point flow and heat transfer for the case of stationary plate, Homann flow, is reached by simplifications of this formulation. Example presented plate velocity functions are exponential, polynomial and co sinusoidal. All kinds of applications of the plate movement is encountered in industry where the stagnation–point flow and heat transfer is involved but our main reason is use of exponential plate velocity function to formulate solidification and melting in these kinds of studies. Velocity and pressure profiles, boundary layer thickness along with temperature profiles have been presented in different physical phenomena governed on this problem. The results obtained show that the more the value of the plate velocity towards the impinging flow, the less the velocity and thermal boundary layer thicknesses will be. Moreover, it was captured that the increase of the Pr number causes the thermal boundary layer thickness to become smaller.

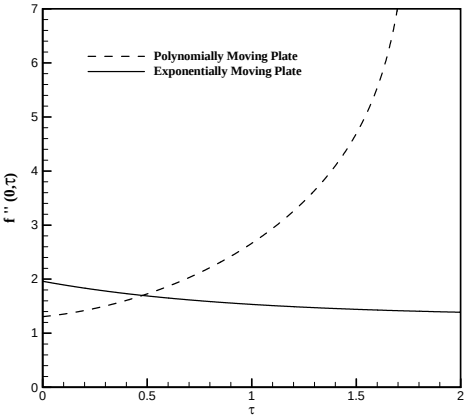

Fig. 18. Distributions of shear stress on the plate for polynomial and exponential plate velocity functions.

REFERENCES

Cunning, G. M., A. M. J. Davis and P. D. Weidman (1998). Radial Stagnation Flow on a Rotating Cylinder with Uniform Transpiration. *J. Eng. Math.* 33, 113-128.

Glauert, M. B. (1956). The Laminar Boundary Layer on Oscillating Plates and Cylinders. *Journal of Fluid Mechanics* 1, 97-110.

Gorla, R. S. R. (1976). Heat Transfer in an Axisymmetric Stagnation Flow on a Cylinder. *Applied Science Research* 32, 541-553.

Gorla, R. S. R. (1977). Unsteady Laminar Axisymmetric Stagnation Flow over a Circular Cylinder. *Developments in Mechanics* 9, 286-288.

Gorla, R. S. R. (1978). Nonsimilar Axisymmetric Stagnation Flow on a moving Cylinder. *International Journal of Engineering Science* 16, 392-400.

Gorla, R. S. R. (1978). Transient Response Behavior of an Axisymmetric Stagnation Flow on a Circular Cylinder Due to Time-Dependent Free Stream Velocity. *Lett. Appl. Eng. Sci.* 16, 493-502.

Gorla, R. S. R. (1979). Unsteady Viscous Flow in the Vicinity of an Axisymmetric Stagnation-Point on a Cylinder. *International Journal of Engineering Science* 17, 87-93.

Griffith, A. and F. Meredith (1936). The Possible Improvement in Aircraft Performance Due to the Use of Boundary Layer Suction. *Royal Aircraft Establishment Report* 3501, 12.

Grosch, C. E. and H. Salwen (1982). Oscillating Stagnation-point Flow. *Proceeding of Royal Society of London*, A 384, 175-190.

Hiemenz, K. (1911). Boundary Layer for a Homogeneous Flow around a Dropping Cylinder. *Dinglers Polytechnuc Journal* 326, 321-324.

Homman, F. Z. (1936). Der EINFLUSS GROSSER Zanhighkeit bei der strmung um den Zylinder und um die Kungel. *Zeitschrift fuer angewandte Mathematik und Mechanik* 16(3), 153–164.

Howarth, L. (1954). The Boundary Layer in Three-Dimensional Flow, Part II: The Flow near Stagnation Point. *Philosophical Magazine* 42, 1433–1440.

Jung, W. L., N. Mangiavacchi and R. Akhavan (1992). Suppression of Turbulence in Wall-Bounded Flows by High-Frequency Spanwise Oscillations. *Physics of Fluids* A 4, 1605-1607.

Kelly, R. E. (1965). The Flow of a Viscous Fluid Past a Wall of Infinite Extent with Time-Dependent Suction. *Quarterly Journal of Mechanics and Applied Mathematics* 18, 287-298.

Mozayyeni, H. and A. B. Rahimi(2013). Three-dimensional Stagnation Flow and Heat Transfer of a Viscous, Compressible Fluid on a Flat Plate. *Journal of Heat Transfer-Transaction of ASME* 135, 101702.1-101702.12.

Rahimi, A. B. and R. Saleh (2007). Axisymmetric Stagnation-Point Flow and Heat Transfer of a Viscous Fluid on a Rotating Cylinder with Time-Dependent Angular Velocity and Uniform Transpiration. *Journal of Fluid Engineering*, 129, 106-115.

Rahimi, A. B. and R. Saleh (2008), Similarity Solution of Unaxisymmetric Heat Transfer in Stagnation-Point Flow on a Cylinder with Simultaneous Axial and Rotational Movements. *Journal of Heat Transfer* 130(5), 054502.1-054502.5.

Saleh, R. and A. B. Rahimi (2004). Axisymmetric Stagnation-Point Flow and Heat Transfer of a Viscous Fluid on a Moving Cylinder with Time-Dependent Axial Velocity and Uniform Transpiration. *Journal of Fluid Engineering* 12, 997-1005.

Shokrgozar, A. and A. B. Rahimi (2009). Three-Dimensional Stagnation Flow and Heat Transfer on a Flat Plate with Transpiration. *Journal of Thermophysics and Heat transfer* 23, 521-513.

Shokrgozar, A. and A. B. Rahimi (2009). Non-axisymmetric Three-dimensional Stagnation-point Flow and Heat Transfer on a Flat Plate. *Journal of Fluids Engineering* 131, 7, 074501.1– 074501.5.

Shokrgozar, A. and A. B. Rahimi (2012). Investigation of Two-dimensional Stagnation-point Flow and Heat Transfer Impinging on a Flat Plate. *Journal of Heat Transfer-Transaction of ASME* 134(6), 064501.1-064501.5.

Stokes, G. (1851). On the Effect of the Internal Friction of Fluids on the Motion of Pendulum. *Transactions of the Cambridge Philosophical Society* 9(2), 8-106.

Stuart, J. T. (1954). On the Effects of Uniform Suction on the Steady Flow Due to a Rotating Disk. *Quarterly Journal of Mechanics and Applied Mathematics* 7, 446-457.

Stuart, J. T. (1955). A Solution of The Navier-Stokes and Energy Equations Illustrating the Response of Skin Friction and Temperature of an Infinite Plate Thermometer to Fluctuations in the Stream Velocity. *Proceedings of the Royal Society London* 231, 116-130.

Stuart, J. T. (1959). The Viscous Flow Near a Stagnation-point When the External Flow Has Uniform Vorticity. *Journal of Aero/Space Science* 26, 124-125.

Takhar, H. S., A. J. Chamkha and J. Nath (1999). Unsteady Axisymmetric Stagnation-Point Flow of a Viscous Fluid on a Cylinder. *International Journal of Engineering Science* 37, 1943-1957.

Wang, C. Y. (1974). Axisymmetric Stagnation Flow on a Cylinder. *Q. Appl. Math.*, 32, 207-213.

Wang, C. Y. (1989). Shear Flow Over a Rotating Plate. *Applied Scientific Research* 46, 89-96.

Wang, C. Y. (1973). Axisymmetric Stagnation Flow Towards a Moving Plate. *American Institute of Chemical Engineering Journal*, 19(5), 1080-1082.

Weidman, P. D. (2012). Non-axisymmetric Homman stagnation-point flows. *J. Fluid Mech.* 702, 460-469.

Zhong, Y. and T. Fang (2011). Unsteady Stagnation-point Flow Over a Plate Moving Along the Direction of Flow Impingement.

International Journal of Heat and Mass Transfer 54, 3103–3108.

Appendix

Using the Navier- Stokes and Energy equation and similarity transformations defined in the text, we have:

(I) R-Momentum Equation:

$$\frac{\partial u}{\partial t} = r\frac{\partial a}{\partial t} f' - \left(\frac{a_o}{\upsilon}\right)^{\frac{1}{2}} ra(t)\dot{S}(t) f'' \tag{1}$$

$$u\frac{\partial u}{\partial r} = a^2(t) r (f')^2 \tag{2}$$

$$w\frac{\partial u}{\partial z} = -2ra^2(t) ff'' \tag{3}$$

$$\frac{\partial^2 u}{\partial r^2} = 0 \tag{4}$$

$$\frac{1}{r}\frac{\partial u}{\partial r} = \frac{1}{r} a(t) f' \tag{5}$$

$$\frac{u}{r^2} = \frac{1}{r} a(t) f' \tag{6}$$

$$\frac{\partial^2 u}{\partial z^2} = \frac{a_o}{\upsilon} a(t) rf''' \tag{7}$$

Using dimensionless parameters defined in relation (12), the following equation is obtained,

$$\begin{aligned} &a_\circ\sqrt{a_\circ\upsilon}\,\xi\frac{\partial\tilde{a}}{\partial\tau} f' - a_\circ\sqrt{a_\circ\upsilon}\,\xi\tilde{a}\tilde{\dot{S}} f'' \\ &+ a_\circ\sqrt{a_\circ\upsilon}\,\xi\tilde{a}^2 f'^2 - 2a_\circ\sqrt{a_\circ\upsilon}\,\xi\tilde{a}^2 ff'' \\ &= -a_\circ\sqrt{a_\circ\upsilon}\frac{\partial\tilde{P}}{\partial\xi} + a_\circ\sqrt{a_\circ\upsilon}\,\xi\tilde{a} f''' \end{aligned} \tag{8}$$

By dividing both sides to the term $a_0\sqrt{a_0\upsilon}\xi\tilde{a}$, it can be achieved that,

$$\begin{aligned} &f''' + (\tilde{\dot{S}} + 2\tilde{a}f) f'' + \left(-\tilde{a}f' - \frac{1}{\tilde{a}}\frac{\partial\tilde{a}}{\partial\tau}\right) f' \\ &- \frac{1}{\tilde{a}\xi}\frac{\partial\tilde{P}}{\partial\xi} = 0 \end{aligned} \tag{9}$$

(II) Pressure Equation:

$$\frac{\partial w}{\partial r} = 0 \;\Rightarrow\; u\frac{\partial w}{\partial r} = \frac{\partial^2 w}{\partial r^2} = 0 \tag{10}$$

$$\frac{\partial w}{\partial t} = -2\sqrt{\upsilon/a_\circ}\frac{\partial\tilde{a}}{\partial\tau} f + 2\dot{S}(t)a(t) f' \tag{11}$$

$$w\frac{\partial w}{\partial z} = 4\left(\frac{\upsilon}{a_o}\right)^{\frac{1}{2}} a^2(t) ff' \tag{12}$$

$$\frac{\partial^2 w}{\partial z^2} = -2\left(\frac{a_o}{\upsilon}\right)^{\frac{1}{2}} a(t) f'' \tag{13}$$

Using dimensionless parameters defined in relation (12), the following equation is obtained,

$$\begin{aligned} &-2a_\circ\sqrt{a_\circ\upsilon}\frac{\partial\tilde{a}}{\partial\tau} f + 2a_\circ\sqrt{a_\circ\upsilon}\tilde{\dot{S}}\tilde{a} f' \\ &+ 4a_\circ\sqrt{a_\circ\upsilon}\,\tilde{a}^2 ff' = -a_\circ\sqrt{a_\circ\upsilon}\frac{\partial\tilde{P}}{\partial\eta} \\ &- 2a_\circ\sqrt{a_\circ\upsilon}\,\tilde{a} f'' \end{aligned} \tag{14}$$

By omitting the term $a_o\sqrt{a_o\upsilon}$ from both sides and, then, integrating with respect to η, we have:

$$\begin{aligned} \tilde{P} = &-2\tilde{a}(\tilde{a}f^2 + f' + \tilde{\dot{S}}f) \\ &+ \int_0^\eta 2\frac{\partial\tilde{a}}{\partial\tau} f d\eta + h(\xi) \end{aligned} \tag{15}$$

Where $h(\xi)$ is the integration constant in which ξ is dimensionless form of r-direction.

As it can be seen from the relation (15), $\partial P/\partial\xi = dh/d\xi$ and both these two terms are independent of η.Hence, in order to find $h(\xi)$, inviscid momentum equation at r-directions will be used utilizing the velocity components in the potential region.

Employing the inviscid r-momentum terms gives,

$$\frac{\partial u}{\partial t} = r\frac{da(t)}{dt} \tag{16}$$

$$u\frac{\partial u}{\partial r} = a^2(t) r \tag{17}$$

$$w\frac{\partial u}{\partial z} = 0 \tag{18}$$

By using dimensionless parameters defined in the relation (12), the r-momentum equation is rewritten as follow,

$$\begin{aligned} &a_\circ\sqrt{a_\circ\upsilon}\,\xi\frac{\partial\tilde{a}}{\partial\tau} + a_\circ\sqrt{a_\circ\upsilon}\,\xi\tilde{a}^2 \\ &= -a_\circ\sqrt{a_\circ\upsilon}\frac{\partial\tilde{P}}{\partial\xi} \end{aligned} \tag{19}$$

By omitting the term $a_o\sqrt{a_o\upsilon}$ from both sides, it is achieved that,

$$\frac{\partial\tilde{P}}{\partial\xi} = \frac{dh}{d\xi} = -\frac{d\tilde{a}}{d\tau}\xi - (\tilde{a})^2\xi \tag{20}$$

$$\Rightarrow\; h(\xi) = -\frac{d\tilde{a}}{d\tau}\frac{\xi^2}{2} - (\tilde{a})^2\frac{\xi^2}{2} + Const. \tag{21}$$

As we know, the pressure at $\eta = \xi = 0.0$ is recognized as the stagnation pressure $P_\circ$. So, it can

be easily found out that $Cosnt. = P_{\circ}$. According to the explanations mentioned above, the final relation of the dimensionless pressure is achieved as,

$$\tilde{P} - \tilde{P}_{\circ} = -2\tilde{a}(\tilde{a}f^2 + f' + \tilde{\tilde{S}}f) + \int_0^{\eta} 2\frac{\partial \tilde{a}}{\partial \tau} f d\eta - \frac{\xi^2}{2}\left(\frac{\partial \tilde{a}}{\partial \tau} + \tilde{a}^2\right) \quad (22)$$

(III) Energy Equation

$$\frac{\partial T}{\partial r} = 0 \Rightarrow \quad u\frac{\partial T}{\partial r} = \frac{\partial^2 T}{\partial r^2} = 0 \quad (23)$$

$$\frac{\partial T}{\partial t} = -\left(\frac{a_o}{\upsilon}\right)^{\frac{1}{2}} (T_w - T_\infty)\dot{S}(t)\theta' \quad (24)$$

$$w\frac{\partial T}{\partial z} = -2(T_w - T_\infty)a(t) f \theta' \quad (25)$$

$$\frac{\partial^2 T}{\partial z^2} = \frac{a_o}{\upsilon}(T_w - T_\infty)\theta'' \quad (26)$$

By applying the dimensionless parameters defined in the relation (12) and eliminating the extra terms from both sides, it can be achieved the energy equation as bellow,

$$\theta'' + \left(\tilde{\dot{S}}(\tau) + 2\,\tilde{a}\, f\right) \mathrm{Pr}.\theta' = 0 \quad (27)$$